Non-Linear Fracture

Recent Advances

Non-Linear Fracture

Recent Advances

edited by

W. G. KNAUSS and A. J. ROSAKIS

Graduate Aeronautical Laboratories,
Caltech, Pasadena, Calif., U.S.A.

Reprinted from *International Journal of Fracture*, Vol. 42, Nos. 1–4 (1990)

Kluwer Academic Publishers
Dordrecht / Boston / London

Library of Congress Cataloging-in-Publication Data

CIP

ISBN 07923-0658-9

Published by Kluwer Academic Publishers,
P.O. Box 17, 3300 AA Dordrecht, The Netherlands.

Kluwer Academic Publishers incorporates
the publishing programmes of
D. Reidel, Martinus Nijhoff, Dr W. Junk and MTP Press.

Sold and distributed in the U.S.A. and Canada
by Kluwer Academic Publishers,
101 Philip Drive, Norwell, MA 02061, U.S.A.

In all other countries, sold and distributed
by Kluwer Academic Publishers Group,
P.O. Box 322, 3300 AH Dordrecht, The Netherlands.

Printed on acid-free paper

Printed in the Netherlands

Foreword

From time to time the *International Journal of Fracture* has presented special matters thought to be of interest to its readers. In previous issues, for example, Dr. H.W. Liu as Guest Editor assembled a series of review papers dealing with fatigue processes and characteristics in metals and non-metals (December 1980 and April 1981). Five years ago Guest Editor W.G. Knauss collected works dealing with dynamic fracture (March and April 1985). Continuing this policy, Dr. W.G. Knauss and Dr. A.J. Rosakis of the California Institute of Technology as Guest Editors have now organized an extensive set of papers concerning the influence of non-linear effects upon the mechanics of the fracture process.

This collection is based upon contributions to a relatively small international Symposium on Non-Linear Fracture Mechanics held under the auspices of the International Union of Theoretical and Applied Mechanics (IUTAM) and convened at the California Institute of Technology in March 1988. It should be noted that although the description of non-linear fracture inherently encompasses a strong material science component, this aspect is not heavily emphasized in the ensuing papers due to the intentional focus upon mechanics.

Volume 42 of the *International Journal of Fracture* will therefore, in successive issues, deal respectively with topics in (1) Damage, (2) Interfaces and Creep, (3) Time Dependence, and (4) Continuum Plasticity. On behalf of the editors and publishers, I wish to express our appreciation to Dr. Knauss, Dr. Rosakis, and their colleagues for their collective efforts.

M.L. WILLIAMS
Editor-in-Chief

Pittsburgh, Pennsylvania
January 1990

Preface

The analysis of material failure has traditionally followed two investigative paths: one was concerned with continuum analyses at the macroscopic size scale and the other with material aspects at the microscopic level. The former attempted to develop a predictive framework for structural failure through continuum concepts in terms of states of ultimate stress or strain, while the latter aimed at better understanding the physical properties of materials needed by the continuum analyst for failure prediction as well as clarifying the microscopic phenomena controlling macroscopic fractures, e.g. dislocations, slip, intergranular and interfacial separations.

A major contribution to failure prediction was the recognition that A.A. Griffith's flaw concepts had wider applicability than to strictly brittle solids. This realization evolved, via M.L. Williams' and G.R. Irwin's contributions, to what has become known as "linearly elastic fracture mechanics". This discipline of solid mechanics has offered a momentous contribution to our ability of coping effectively with a large class of fracture problems. It provides a single principal parameter for characterizing the onset of fracture, the stress intensity factor, with attendant crack tip characteristics such as the energy release rate concept and the idea of stress field autonomy at the crack front. In particular, the latter concept allowed the scaling connection between laboratory fracture tests and full scale service structures, a feature of the theory that is likely to survive only into a limited set of non-linear fracture formulations.

With time and through greater analytical flexibility via numerical computations it became also increasingly clear that linearly elastic description of fracture could not do justice to the large variety of materials of interest in engineering. Accordingly, the last decade has seen growing efforts at incorporating more detailed microstructural material description into continuum formulations of crack growth problems. Such developments make primarily increased use of non-linear, macroscopic constitutive descriptions in the form of continuum plasticity, rate and temperature sensitivity, and with more complicated phenomena such as stress-induced phase transformations, for example. Although fracture problems are still mostly based on small strain deformation fields, relevant studies begin to recognize that large strains and finite rotations in the crack tip vicinity are needed in a kinematically consistent and "fully" non-linear framework.

Beyond the more macroscopic considerations of material constitution a trend is now developing to describe in greater detail the failure processes at the microscopic level around the crack tip in terms of so-called "damage"; these processes include phase separations, slip, and intergranular microcracks that transform into growing voids. Although these characteristics can occur away from the crack tip, they are usually associated with the process zone, that is, in the small region where the actual fracture process takes place.

The discipline of non-linear fracture mechanics which incorporates these material aspects has as its primary goal a more physics-based continuum formulation of crack tip problems than the linear theory could provide. However, beyond this immediate differentiation there is implicit in this new development an attempt to describe the complete material response in its transition from the continuum to the damaged and failing material. One thus aims at describing the complete fracture process in terms of material characterization and continuum fields without recourse to "arbitrary" fracture criteria. The goal is thus to replace the stress intensity factor or the fracture energy as the global fracture parameter(s) of linear fracture mechanics by a local material intrinsic parameter.

If such a formulation were possible fracture mechanics would have passed, historically, through three stages of development: starting from the classical failure analysis of continua during the first quarter of this century which was based on local (principal) stress or strain criteria, the next phase is identified with linearly elastic fracture mechanics in which stress singularity characterization induced by the crack geometry dominated the failure description. We are then presently moving into a third phase, distinguished by a fully non-linear description of the material and the failure process, and wherein the crack or flaw provides only the high stress or strain field gradients within which a local, material-based failure criterion can be satisfied at the crack tip.

That such questions cannot be addressed without detailed and careful experimental work is clear. Indeed, experimental work is pivotal in all stages of such developments related to (1) constitutive formulations, (2) their application in fracture problems and (3) the elucidation of the physical processes that serve to augment our notions of how the fracture process develops. It is simultaneously clear that, in order to deal with the increased consideration of detail, such experimental work will also have to deal with ever increasing spatial and temporal resolution of physical quantities in experiments. In this sense the experimental mechanics of non-linear fracture problems will have to move closer to the domain of the material scientist and encompass the emerging discipline that is often called "the mechanics of materials."

The symposium content has been grouped loosely into four sections under the headings of Damage, Interfaces and Creep, Time Dependence, and Continuum Plasticity. While the grouping could not be made altogether precise, we have attempted to represent the main thrust of the contributions in a coherent setting.

Damage occurs in different forms: in pure polycrystalline solids a major contribution to the deformation can arise from slip formation within grains as well as from the development of intergranular cracks. Moreover, inclusions can precipitate interfacial separations that develop into voids. In polymers the generation of micro-flaws in the form of crazes and of submicron discontinuities provides a similar damage profile. These damage phenomena are connected to clearly identifiable processes, and considerations along these lines are represented in the first five of the papers. There is, however, an alternate and less physics-specific view which derives basically from a continuum description in the form of a damage function without necessarily specifying an accompanying physical process. In this approach to constitutive description of damaged materials one postulates a (possibly tensorial) damage function which accounts for progressive softening of the material with strain or time. The evaluation of this function needs to be accomplished essentially in terms of macroscopically measured changes in material rigidity, as illustrated in several contributions.

Interfacial separation and creep play possibly interactive roles in macroscopic material response. Unbonding of inclusions is an important aspect of failure behavior of the emerging composite materials. It appears that the somewhat disturbing oscillatory character of the asymptotic stress and displacement fields for interface cracks in linearized elasticity is less troublesome when nonlinear material characteristics and large deformations operate. Several contributions address this issue. Another issue intimately coupled with damage development is the occurence of creep. This phenomenon may be the result of intrinsic time-dependent processes at the atomic level, but it is also occasioned by the time-dependent development of microscopic damage. Incorporation of such damage evolution generates non-linear time or rate-dependent constitutive behavior; damage-induced creep can again be represented either in terms of physically identified mechanisms or in terms of a phenomenological damage function. Several contributions examine the effect of this type of material description on the stress distribution around the tips of cracks. In this context it is not clear what differences separate non-linearly viscoelastic and the traditional creep representations of material

behavior, except primarily historical associations.

Another group of papers deals with non-linear effects on dynamic crack propagation, addressing both stress wave loading on stationary cracks as well as rapidly propagating cracks (up to 60% of the Rayleigh wave speed). While major advances in the past contributed analytical (linearly) elastodynamic solutions to this topic, the present papers emphasize understanding the influence and interplay of inertia, plasticity, rate sensitivity and adiabatic heat generation on the deformation field around initiating, running and arresting crack tips. These problem parameters control whether fracture localized at the crack tip favors separation through void growth or whether it is dominated by low energy cleavage. This topic is of considerable interest, because such material behavior would establish a main source for different toughness measures experienced in static versus dynamic situations. Answers to this and related questions require extensive experimental work in order to elucidate the true physical situation before proper analytical modelling can be achieved. In fact, analytical studies in dynamic fracture have benefitted from close interaction with experimental investigation.

To round out the presentation, a sequence of papers addresses non-linear continuum description of the near tip deformations, primarily in terms of asymptotic solutions based on plasticity for stationary and quasi-statically propagating cracks. In spite of considerable mathematical difficulties associated with analytical solutions for (incremental) plasticity formulations, progress is being made in several areas. These include use of anisotropic plasticity for cracks in single crystals as well as crack growth under large scale yielding. An essential ingredient in these studies is the coupling of analytical developments with large scale computational efforts, as well as experimental progress in addressing the near tip deformation field in the presence of plasticity.

W.G. KNAUSS
A.J. ROSAKIS

TABLE OF CONTENTS

International Journal of Fracture **42**: 1–19, 1990.
W.G. Knauss and A.J. Rosakis (eds) Non-linear Fracture.

Finite element analysis of void growth in elastic-plastic materials

R.M. McMEEKING and C.L. HOM
Department of Materials and Department of Mechanical Engineering, University of California, Santa Barbara, CA 93106, USA

Received 1 August 1988; accepted 15 August 1988

Abstract. Three-dimensional finite element computations have been carried out for the growth of initially spherical voids in periodic cubic arrays and for initially spherical voids ahead of a blunting mode I plane strain crack tip. The numerical method is based on finite strain theory and the computations are three-dimensional. The void cubic arrays are subjected to macroscopically uniform fields of uniaxial tension, pure shear and high triaxial stress. The macroscopic stress-strain behavior and the change in void volume were obtained for two initial void volume fractions. The calculations show that void shape, void interaction and loss of load carrying capacity depend strongly on the triaxiality of the stress field. The results of the finite element computation were compared with several dilatant plasticity continuum models for porous materials. None of the models agrees completely with the finite element calculations. Agreement of the finite element results with any particular constitutive model depended on the level of macroscopic strain and the triaxiality of the remote uniform stress field. For the problem of the initial spherical voids directly ahead of a blunting mode I plane strain crack tip, conditions of small scale yielding were assumed. The near tip stress and deformation fields were obtained for different void-size-to-spacing ratios for perfectly plastic materials. The calculations show that the holes spread towards the crack tip and towards each other at a faster rate than they elongate in the tensile direction. The computed void growth rates are compared with previous models for void growth.

1. Void growth

For progress in understanding both the phenomenon of ductile fracture and the process of non-isostatic pressing, it is desirable to have models for the growth/collapse of voids in arbitrary states of stress. McClintock [1] developed growth predictions for cylindrical voids, while later Rice and Tracey [2] obtained results for spherical holes by minimizing a functional of the velocity field. The model for spherical holes was later improved by Budiansky, Hutchinson and Slutsky [3]. The solutions show the strong effect of stress triaxiality on the rate of growth. In the latter two cases, the analysis was carried out for a single void in an infinite matrix and so the results are valid only for a porosity which is a small fraction of the whole. On the other hand, Needleman [4] and Tvergaard [5] treated cylindrical holes in a square array subject to a macroscopically uniform state of stress. They used the finite element method to obtain the solutions. Interactions between voids are apparent in the velocity fields and the local stress distributions. The coupling is probably stronger in these two-dimensional problems than in the interactions between initially spherical voids. In an attempt to understand such three-dimensional effects, Andersson [6] and Tvergaard [7] used the finite element method to analyze the growth of a spherical void in a high triaxial stress state constrained to axially symmetric deformation in a cylinder. Because of the constraint, the implied interaction between neighboring voids is still strong. Hancock [8] has used similar calculations

of axisymmetric deformations to study void–void interactions and observed that there are strong couplings between voids on the 45 degree planes.

Another approach to modelling void growth extends the Rice and Tracey approach by using the same method applied to spherical cells containing spherical holes. This technique was used by Gurson [9, 10] to study the behavior of voids in high volume fractions for a variety of states of stress. At low volume fractions the results agree with those of Rice and Tracey [2]. The rate of dilatation of the voids was determined by Gurson [9, 10] and presented in indirect form because the main purpose was to obtain a yield condition and an associated flow law for a macroscopic composite containing a volume fraction of spherical voids. Modifications of these laws were developed by Tvergaard [5, 7] to improve their agreement with calculations of bifurcation into shear banding in square arrays of cylindrical holes and axisymmetric spherical holes.

There is little work on comparing these constitutive laws for porous ductile materials with experimental data. Bourcier, Koss, Smelser, and Richmond [11] have shown that partially densified powder metallurgy specimens of Ti and Ti–6Al–4V have lower flow stresses than predicted by the models of Gurson [9, 10] and Tvergaard [5, 7]. Similarly, Richmond [12] has data for iron confirming this overprediction. Based on these data for Ti, Ti–6Al–4V and iron and on considerations of yielding in shear of a material containing a cubic array of spherical voids, Richmond and Smelser [13] have devised an alternative yield function and a corresponding flow law which agrees with the experimental data.

In this paper, the behavior of initially spherical holes in cubic arrays analyzed by a large deformation finite element technique is reviewed. This work follows on from the initial effort of Harren [14] and was carried out by Hom and McMeeking [15]. A representative fraction of a unit cell was treated with appropriate symmetry and periodic conditions to produce macroscopically homogeneous deformation. The full three-dimensional interactions between voids were accounted for, and a moderate and high volume fraction of the voids were studied. Simple shear, uniaxial tension and a state of high triaxiality were applied in the calculations. The results are compared with the models of Gurson [9, 10], Tvergaard [5, 7] and Richmond and Smelser [13] in an attempt to assess which conforms most closely to the finite element calculations.

2. Problem formulation for cubic array of voids

A cubic array of initially spherical voids in an infinite elastic–plastic body was considered. The void sizes and spacings were chosen to give two initial porosities of 6.5 and 0.82 percent. The material was originally stress free and monotonically increasing principal stresses were applied to the infinite body in such a manner that they were aligned with the axes of the cubic array. The states of stress were macroscopically homogeneous and accounted for pure shear, uniaxial tension and an axisymmetric state of high triaxiality in which the lateral stresses are 70 percent of the tensile axial stress.

The matrix material surrounding the voids was elastically isotropic subject to yielding governed by the Von Mises criterion with σ_f taken as the true flow stress in uniaxial tension. Isotropic strain hardening was used with a power law form given by

$$\left(\frac{\sigma_f}{\sigma_0}\right)^{1/N} - \left(\frac{\sigma_f}{\sigma_0}\right) = \frac{3G\bar{\varepsilon}^p}{\sigma_0} \tag{1}$$

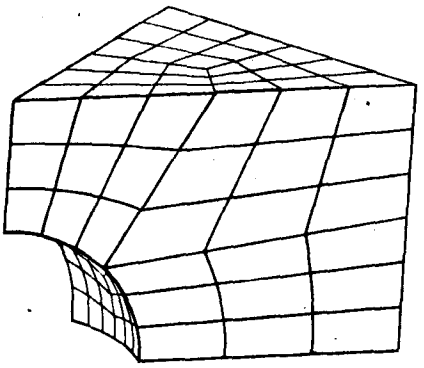

Fig. 1. Typical finite element mesh used to model the one-sixteenth cell of the void-matrix aggregate.

where σ_0 is the initial yield stress, G is the elastic shear modulus and $\bar{\varepsilon}^p$ is the tensile equivalent plastic strain.

Because of the periodic arrangement of the voids, it was sufficient to consider only a single unit cell consisting of a cube containing one void. Each cell deforms into a right parallelopiped due to imposed velocities on the boundary. The evolving shape was determined by the state of stress: The technique of Needleman [4] was used to ensure the correct state of stress. This technique consists of adjusting the uniform normal displacement increments of each face of the unit cell to ensure that the average true stress on each face maintains the desired level. However, a reduction of the size of the problem was possible due to symmetries. In the axisymmetric states of uniaxial stress and high triaxiality it was necessary to solve the problem in only one-sixteenth of the cubic unit cell [15]. In pure shear, the one-sixteenth segment and its neighbor across the diagonal plane must be used. For more detail see [15], where the same results are reported in greater detail.

Large strains and rotations are allowed for through the finite deformation formulation of McMeeking and Rice [16] as modified and implemented in the ABAQUS [17] finite element code. As such, the method is similar to that developed by Needleman [18] and Osias and Swedlow [19]. The finite element mesh used for the axisymmetric problems is shown in Fig. 1, whereas the mesh for pure shear was simply double that shown. The illustrated mesh has 135 twenty noded isoparametric brick elements and 1084 nodes. The dilatation in the element was represented by extra degrees of freedom and the model was freed from locking overconstraint by a technique based on the method of Nagtegaal, Parks and Rice [20].

The calculations were carried out incrementally up to macroscopic true strains of the order 0.7 for the uniaxial tension state and 0.3 for the pure shear state and the high triaxial stress state. The macroscopic true strain is defined to be $E_3 = \ln(l/l_0)$ where l_0 is the undeformed length of the vertical edge of the unit cell shown in Fig. 1 and l is the current length of that edge. Typically, 50 increments were necessary to obtain macroscopic true strains of the order 0.7 for the uniaxial tension state and 0.3 for the pure shear state and the high triaxial stress state.

3. Results for growth of voids

The finite element calculations were carried out for a power-law hardening matrix material with $E/\sigma_0 = 200$ and $\nu = 0.3$ where E is Young's modulus and ν is Poisson's ratio. The

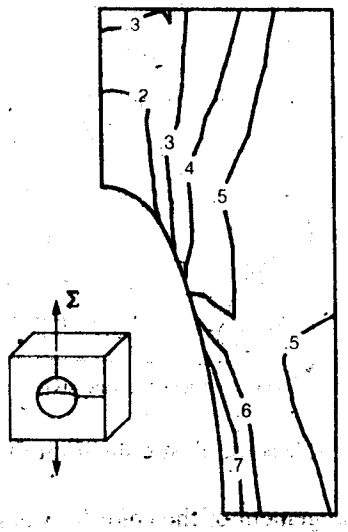

Fig. 2. A contour plot of the equivalent plastic strain $\bar{\varepsilon}^p$ for uniaxial tension at a true strain $E_1 = 0.50$ and $f_i = 6.5\%$ and $N = 0.1$.

uniaxial true stress/logarithmic tensile strain law given by (1) was used with $N = 0.1$. In this section the results for initial void volume fractions f_i of 6.5 and 0.82 percent are presented for the three different loadings.

3.1. Change in void shape

In the case of uniaxial tension, the initially spherical void elongates in the tensile direction with increasing strain. After a tensile true strain of 0.5, the holes are long and narrow and the ligaments between neighboring voids are like columns with a curvilinear cross shape for the section. Figure 2, a contour plot of the equivalent plastic strain for $f_i = 6.5$ percent, shows that the plastic deformation is concentrated in these ligaments. However, little or no void interaction occurs between neighboring voids in the cubic array under uniaxial tension [15]. In this way, the behavior of the initially spherical voids differ greatly from that predicted by Needleman [4] for cylindrical voids in square cells under plane strain tension. Needleman found that after a stage of transverse contraction, the cylindrical holes start to grow laterally with high strains developing in the ligaments. This change in behavior in the two-dimensional problem occurs at a moderate strain of 0.3. Therefore it seems that the interaction of transverse neighbors is stronger for cylindrical voids than for spherical voids.

In the case of pure shear, the voids elongate in the tensile direction and contract in the compressive direction, but the void volume fraction remains almost exactly constant throughout the whole load history. Figure 3 is a contour plot of $\bar{\varepsilon}^p$ for $f_i = 6.5$ percent. In this case, the maximum effective plastic strain occurs between neighboring voids in the principal shear plane. Unlike uniaxial tension, this maximum does not occur at the void's surface or in the ligament between transverse neighboring voids. Instead, the maximum occurs at the intersection of shear band like features extending from void to void.

In contrast to the low triaxial stress states, when there is high triaxiality, the voids dilate substantially and strong neighbor interaction occurs at relatively low strains. For

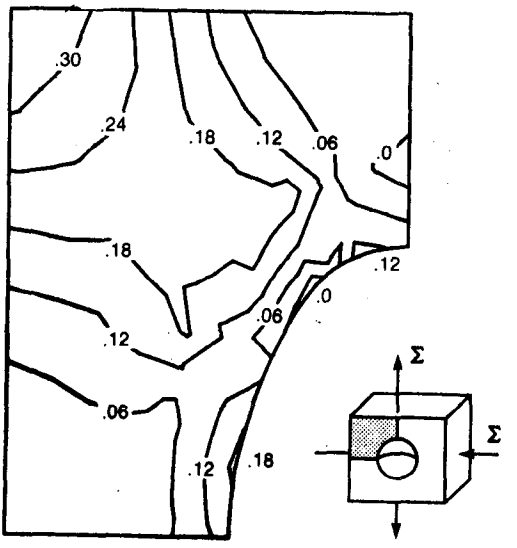

Fig. 3. A contour plot of the equivalent plastic strain $\bar{\varepsilon}^p$ for pure shear at a true strain $E_3 = 0.25$ with $f_i = 6.5\%$ and $N = 0.1$.

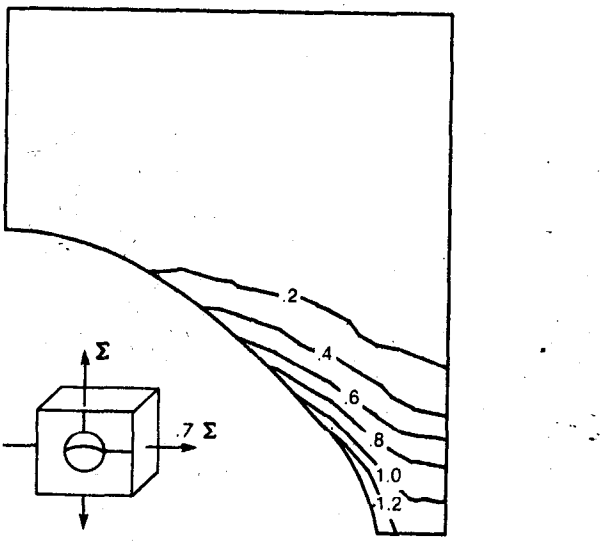

Fig. 4. A contour plot of the equivalent plastic strain $\bar{\varepsilon}^p$ for the high triaxial stress state at true strain $E_3 = 0.25$ with $f_i = 6.5\%$ and $N = 0.1$.

$f_i = 0.82$ percent the void's volume increases steadily and the hole remains roughly spherical in shape. For the higher initial void volume fraction $f_i = 6.5$ percent, the strength of void interaction is more apparent. At a tensile strain of 0.2 the void has started to bulge out towards its transverse neighbor. Figure 4, a contour plot of $\bar{\varepsilon}^p$ for $f_i = 6.5$ per cent, shows that the plastic strains are concentrated in the ligament and are significantly larger than for the low triaxial cases at the same nominal strain. The ligament between voids transverse to the maximum principal stress exhibits necking behavior which indicates that the voids are beginning to interact strongly.

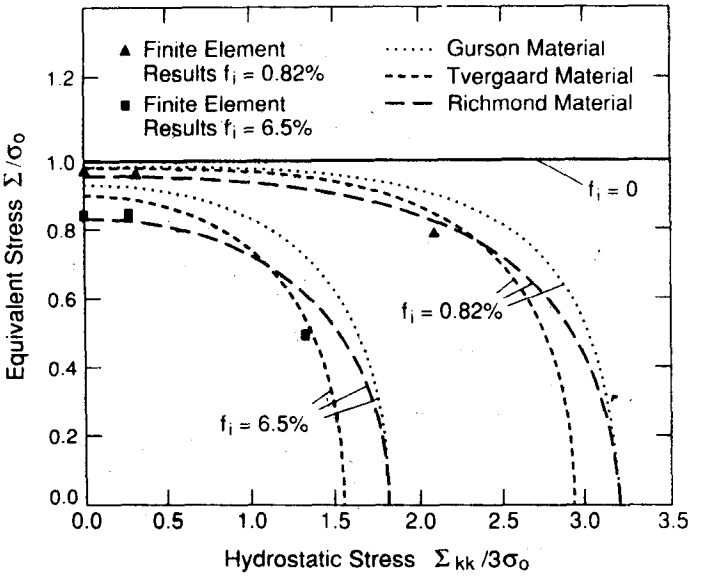

Fig. 5. Limit loads predicted by finite element analysis and yield surfaces of the Gurson, Tvergaard and Richmond models.

3.2. Initial yield predictions

The results of the finite element calculation can be used also to evaluate the accuracy of the existing continuum models for dilatant plastic behavior caused by the presence of voids. One method of comparison is to examine the yield point predicted by the finite element calculations and the Gurson [9, 10], Tvergaard [5, 7] and Richmond [13] models for the three loading conditions. The three models are described together by Hom and McMeeking [15]. The yield point in the finite element calculations is estimated to be at the region of rapid reduction of the tangent stiffness in the load deflection curves. In Fig. 5, the yield surfaces of the continuum models and the yield points predicted by the finite element analysis are plotted in the plane of tensile equivalent stress versus hydrostatic stress. For the low triaxial stress states of pure shear and uniaxial tension, the yield points of the finite element calculations agree best with the Richmond [13] model. This result is interesting since the Richmond model is based on the concept of yielding being concentrated on shear bands at 45 deg to the principal stress directions and is more persuasive in the case of pure shear.

For the high triaxial stress state, the finite element calculations agree better with the Tvergaard [5, 7] and Richmond [13] models. This behavior is not surprising since Tvergaard's modification of Gurson's [9, 10] equation is based partially on axisymmetric finite element results for a high triaxial stress state. In addition, Richmond and Smelser [13] chose their modification of Gurson's [9, 10] law to agree with it in purely hydrostatic stress where both are in accord with the Torre [21] solution.

3.3. Plastic flow behavior

In addition to the yield point calculation, the stress–strain curves of the finite element computations have been used for comparison with the plastic flow characteristics of the

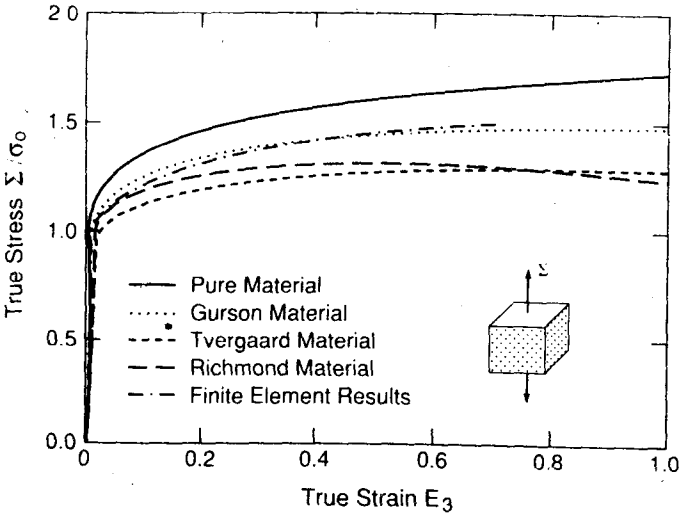

Fig. 6. Comparison of the stress–strain behavior of the finite element analysis and the continuum models for uniaxial tension, with an initial void volume fraction $f_i = 6.5\%$ and a hardening coefficient $N = 0.1$.

continuum models. The results of this comparison depend strongly on the macroscopic stress state. In the low triaxiality cases, where the void volume remains roughly constant, the stress–strain curves of the finite element calculation become relatively stiff at high strains compared to the behavior at low strain and further loss in the material's load carrying capacity due to void growth is negligible. However for the high triaxiality case, rapid void growth causes a substantial decay in the load-deflection curve of the finite element calculation. It was found that this overall type of behavior was not completely described by any particular continuum model.

Figure 6 shows the stress–strain curves predicted by the finite element analysis and the three continuum models for uniaxial tension with $f_i = 6.5$ percent and $N = 0.1$. The finite element computation rapidly diverges from the initial yield prediction of the Richmond model and conforms to the Tvergaard prediction up to about 0.1 true strain. From a strain of 0.2 to about 0.4, the numerical results stiffen toward the Gurson prediction. However, for true strains above 0.4, the finite element model maintains a higher load carrying capacity than for all three continuum models. The behavior of the finite element computation for $f_i = 0.82$ percent is similar to the high porosity case. The results agree with the Tvergaard prediction at low strain, and diverge to the Gurson result with increasing strain. At high strains, a stiff response compared with the continuum models is observed. For uniaxial tension, the voids of the finite element analysis grow at a slower rate than the voids of the continuum models. At high strains, the void volume fraction predicted by the continuum models increases at an accelerating rate while the rate of increase of the void volume fraction predicted by the finite element method seems to be tending towards a low asymptotic value. Since they are idealized to remain spherical, the voids of the continuum theories are modelled as growing in the transverse directions and thus interact strongly with neighboring voids. However, the voids of the finite element solution grow as ellipsoids and give rise to ligaments which only change their cross-sectional area slowly. These ligaments have larger cross-sectional area and are capable of carrying more load than the ligaments surrounding

spherical voids of the same current volume fraction. This determines the difference between the flow stress predictions of the continuum models and the finite element predictions as summarized in Fig. 6. The dominance of void shape change in the finite element results at high strains results in lower void growth rates which in turn results in higher load carrying capacity. This explains why the finite element model does not lose load carrying capacity at high strains like the continuum models. This result indicates that in addition to the void volume fraction, internal variables are required in the continuum models to account for the effect of void shape changes.

As in the uniaxial stress case, the finite element prediction for the stress–strain curve in the pure shear case diverges rapidly from the initial agreement with the Richmond model. At strains larger than 0.01, the agreement between the Tvergaard model and the finite element results is good in the case of $f_i = 6.5$ percent. Even though the finite element prediction of initial yield agrees best with the Richmond model for $f_i = 0.82$ percent, continued straining increases the macroscopic flow stress of the cubic cell until at 0.05 strain the effective value is only slightly lower than the prediction of the Tvergaard model. However, thereafter the trend is for the finite element results to move gradually away from the Tvergaard prediction and back down towards the Richmond model. Overall, though, the Tvergaard model is in best agreement with the finite element calculations.

Unlike the low triaxial stress states, the character of the finite element calculation for the high triaxial stress state depends more on the initial void volume fraction. Figures 7 and 8 show the true stress–strain behavior of the finite element and continuum models with initial porosities of 6.5 and 0.82 percent respectively, both with a strain hardening exponent of 0.1. In each case the finite element calculation reaches a maximum in load in the early stages of straining. For an initial void volume fraction of 6.5 percent, this maximum is followed by a rapid drop in the load carrying capacity compared with the continuum models. However, this sharp drop is not observed in the lower initial porosity material. As noted earlier, in the finite element calculations the voids for the 0.82 percent initial porosity remain spherical while the voids for the 6.5 percent initial porosity bulge out towards their neighbors. It is

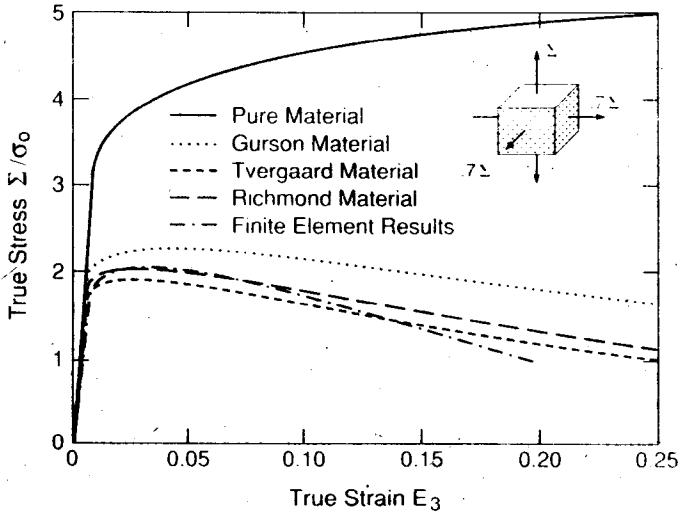

Fig. 7. Comparison of the stress–strain behavior of the finite element analysis and the continuum models for the high triaxial stress state, with an initial void volume fraction $f = 6.5\%$ and a hardening coefficient $N = 0.1$.